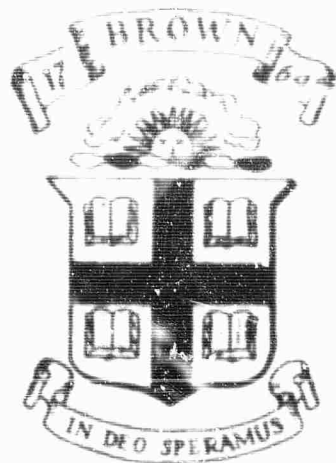


AD609495



Division of Engineering
BROWN UNIVERSITY
PROVIDENCE, R. I.

COPY	2	OF	3	R
HARD COPY	\$ 1.00			
MICROFICHE	\$ 0.50			

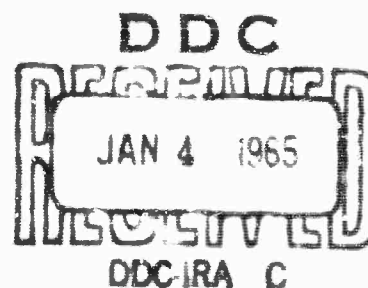
A DIGITAL FERRITE PHASE SHIFTER

25P

A Study of the Differential Phase Shift in
Circular Cylindrical Wave-Guides Containing
Circumferentially Magnetized Ferrite Rods and
Tubes Under Transverse Electric Mode Excitation

BY

D. M. BOLLE and G. S. HELLER



Department of Defense
Advanced Research Projects Agency
Material Research Program

ARPA/E13

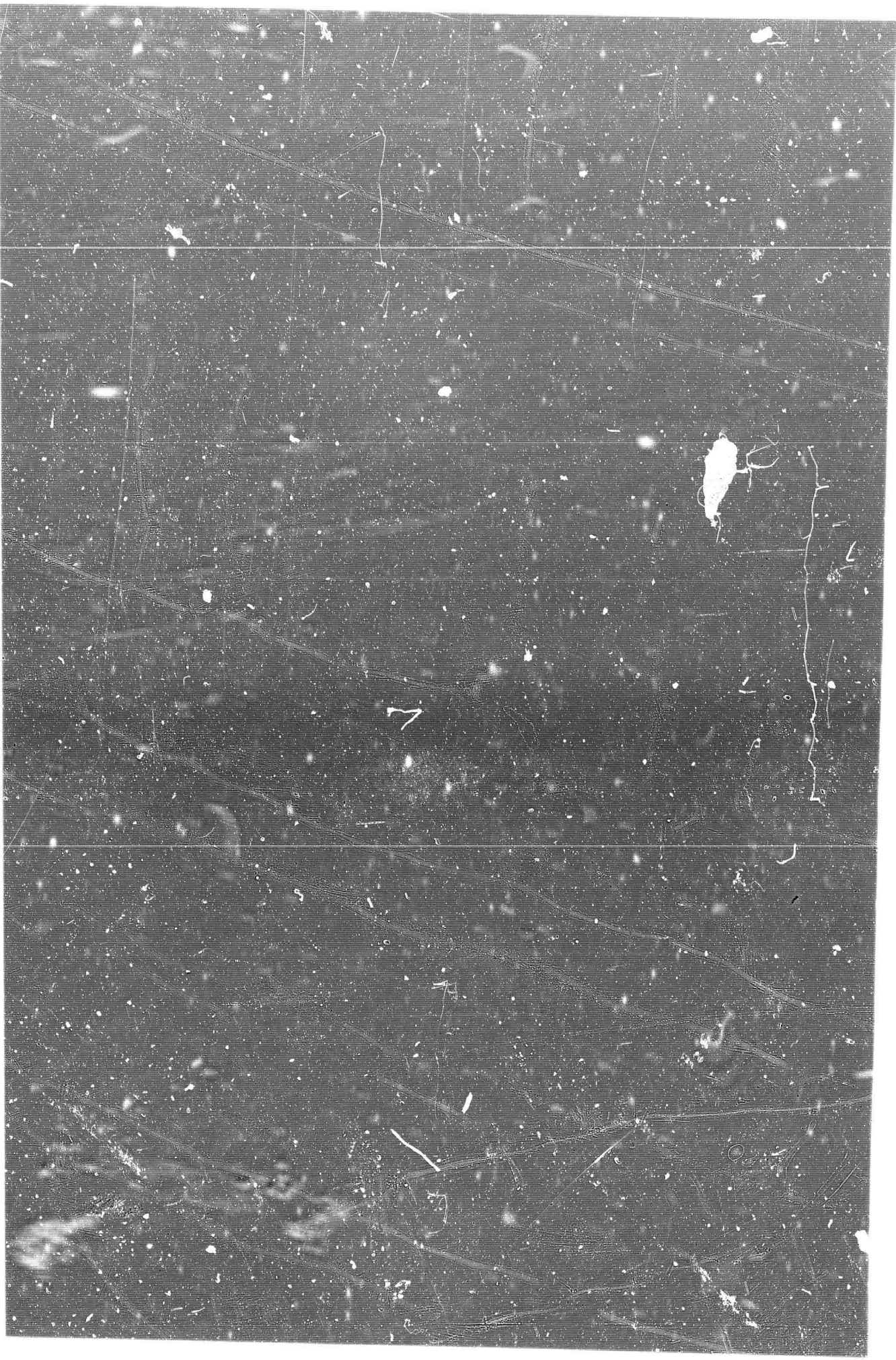
October 1964

ARCHIVE COPY

DISCLAIMER NOTICE

THIS DOCUMENT IS THE BEST
QUALITY AVAILABLE.

COPY FURNISHED CONTAINED
A SIGNIFICANT NUMBER OF
PAGES WHICH DO NOT
REPRODUCE LEGIBLY.



A DIGITAL FERRITE PHASE SHIFTER

A Study of the Differential Phase Shift
in Circular Cylindrical Waveguides Containing
Circumferentially Magnetized Ferrite Rods and Tubes
under Transverse Electric Mode Excitation

by

D. M. Bolle and G. S. Heller

Brown University

Providence, Rhode Island

October 1964

Prepared for

Department of Defense

Advanced Research Projects Agency

Materials Research Program

This research was supported in the main by the Advanced Research Projects Agency under Contract ARPA-E-114, and, in part, by the Air Force Cambridge Research Laboratories under Contract AF 19(628)-2498. This work was reported on at the ICMCI, Tokyo, Japan, September 1964, and was performed in the Millimeter Wave Laboratory, Division of Engineering, Brown University, in a study of material-wave interaction effects.

Introduction

To conserve power and increase the accuracy to which a prescribed phase shift may be set, digital rather than the usual continuously variable type phase shifters have been suggested for use in phased microwave antenna arrays. Various schemes have been suggested including the use of magnetically saturated toroids in rectangular waveguides in which the phase can be shifted digitally by the reversal of the magnetization in the toroid through the application of a current pulse. Many of these arrangements suffer from the disadvantage that not all of the ferrite is effective in producing differential phase shift since only a portion is in the region of circular polarization.

Ferrite toroids in round waveguides utilizing the circular TE mode seem to be the natural microwave structure for such non-reciprocal phase shifters for several reasons⁽¹⁾. First, it is possible to place all of the ferrite in a region of circular polarization so that the entire volume of material is then effective in producing non-reciprocal phase shift. Secondly it is possible to make narrow transverse cuts through such a structure without introducing significant reflection so that a number of these sections may be cascaded to allow d.c. insulation between them. Thirdly, such transverse cuts may be used for the introduction of wires to carry the switching current to the toroids. Finally, a thin wire may be introduced along the waveguide axis without appreciably changing the fields. The ferrite magnetization could then be switched by a current flowing along this wire. Transverse cuts in this center conductor can

(1) The use of the TE_{01} mode in conjunction with circumferentially magnetized ferrite tubes inserted in circular cylindrical guides appears to have been suggested first by A. G. Fox, S. E. Miller and M. T. Weiss, "Behavior and Application of Ferrites in the Microwave Region", Bell Sys. Tech. J., Vol. 34, pp. 5-103, Jan. 1955. The use of such structures as digital phase shifters was proposed by the second author while he was at Lincoln Laboratories, see: Solid State Research, Lincoln Laboratories, Mass. Inst. of Techn., No. 1, Section IV G, pp. 38, 1963.

also be made without disturbing the mode.

The usual microwave ferrite materials may not be suitable for such application since they will require desirable switching, as well as good microwave properties. Such materials are under investigation at this as well as other laboratories.

A theoretical investigation is presented here of the mode structure and the differential phase shift per unit length for the circular cylindrical guide containing a coaxial ferrite tube. While it is recognized that in practice the ferrite toroid will be of finite length and the ferrite will not necessarily be completely magnetically saturated it is expected that this study will yield useful design data such as the differential phase shift, optimum toroid placement and dimensions.

Theory

We will first consider wave propagation in a circular cylindrical guide completely filled with ferrite magnetized in the circumferential or ϕ - direction. The completely filled guide is treated only to study the character of the eigenfunctions and their eigenvalues and it is not expected (due to the difficulty of synthesizing a uniform circumferential magnetizing field) that such an arrangement will have practical utility. The analysis will then be extended to more complex structures such as tubes or rods of ferrite placed coaxially within circular cylindrical guides.

A ferrite magnetized in the direction of the ϕ - coordinate may be characterized by the permeability tensor

$$\mu = \mu_0 \begin{bmatrix} 1+\chi & 0 & j\chi \\ 0 & 1 & 0 \\ -j\chi & 0 & 1+\chi \end{bmatrix} \quad (1)$$

where

$$\chi = \frac{\gamma M \gamma_H}{(\gamma_H)^2 - \omega^2} \quad \kappa = - \frac{\omega \gamma M}{(\gamma_H)^2 - \omega^2} \quad (2)$$

and γ is the gyromagnetic ratio, M the magnetization and H the magnetizing field. We will restrict our attention to those TE modes that exhibit rotational symmetry. Assuming time and axial variations of the form $e^{j\omega t}$ and $e^{-j\beta z}$, respectively, we find that the only non-vanishing component of the electric field E_ϕ must satisfy the differential equation

$$\frac{d^2 E_\phi}{dr^2} + \frac{1}{r} \frac{dE_\phi}{dr} + \left(k^2 + \frac{a'}{r} - \frac{1}{r^2} \right) E_\phi = 0 \quad (3)$$

where r is the radial coordinate and

$$\alpha' = \beta x / (1 + x)$$

$$k^2 = \omega^2 \mu_o \epsilon \Delta' - \beta^2 \quad (4)$$

$$\Delta' = [(1+x)^2 - x^2] / (1+x)$$

The components of the magnetic field are given by

$$H_r = - \frac{\beta(1+x)}{\gamma_o^2} E_\phi + \frac{x}{\gamma_o^2} \frac{1}{r} \frac{\partial}{\partial r} (r E_\phi) \quad (5)$$

$$H_z = - \frac{j\beta x}{\gamma_o^2} E_\phi + j \frac{(1+x)}{\gamma_o^2} \frac{1}{r} \frac{\partial}{\partial r} (r E_\phi)$$

where

$$\gamma_o^2 = \omega^2 \mu_o [(1+x)^2 - x^2] = \omega^2 \mu_o \Delta \quad (6)$$

We seek solutions to (3) subject to the boundary condition

$$E_\phi = 0, \quad r = b \quad (7)$$

where b is the inner radius of the guide.

Equation (3) is recognized as Tricomi's form of the Confluent Hypergeometric equation⁽²⁾. We may thus construct solutions using Humbert's or Whittaker's notation or other forms of the Confluent Hypergeometric functions⁽³⁾. Since the tabulation of these functions and their eigenvalues is not complete it was decided to construct solutions that relate directly to Bessel and Neumann functions. This was prompted by the fact that as α' goes to zero (3) reduces to Bessel's equation. Further, as α'

(2) -----
Bateman Compendia, McGraw-Hill 1953, Vol. 1, p. 251.

(3) Morse, P. M. and Feshbach, H., Methods of Theoretical Physics, McGraw-Hill 1953, Vol. 1, pps. 604-619.

is proportional to the product $\beta\alpha$ we have that the eigenvalues must reduce to those of the Bessel functions, both at cut-off $\beta = 0$, and as α goes to 0, i.e., as the ferrite material is allowed to become isotropic. Thus constructing solutions $B_1(\alpha;kr)$ and $H_1(\alpha;kr)$ not only facilitated the computational work but also aided in physical interpretation.

Thus

$$B_1(0;x) = J_1(x), \quad H_1(0;x) = N_1(x) \quad (8)$$

where $x = kr$.

These functions are given by

$$B_1(\alpha;x) = \sum_{p=0}^{\infty} a_p x^{p+1}$$

$$a_{p+2} = -(\alpha a_{p+1} + a_p)/(p+2)(p+4) \quad (9)$$

$$a_0 = 1/2, \quad a_1 = -\alpha/3$$

and

$$H_1(\alpha;x) = \frac{2}{\pi} \left\{ \left[\gamma + \ln \left(\frac{x}{2} \right) \right] B_1(\alpha;x) - \frac{1}{(1+\alpha^2)x} - \frac{\alpha}{1+\alpha^2} \right. \\ \left. + \sum_{n=0}^{\infty} d_{n+2} x^{n+1} \right\} \quad (10)$$

$$d_{n+2} = -(\alpha d_{n+1} + d_n)/n(n+2) - [1/n + 1/(n+2)]a_n$$

$$d_0 = -1/(1+\alpha^2), \quad d_1 = -\alpha/(1+\alpha^2), \quad d_2 = (\gamma - \ln^2 - 1/2)/2$$

where

$$\alpha = \alpha'/k$$

Figures 1 through 4 show the functions $B_1(\alpha; x)$, $H_1(\alpha; x)$ and their derivatives as a function of x with α as a parameter ($-2 \leq \alpha \leq 10$; $0 \leq x \leq 10$). The solution to equation (3) may thus be written in the form

$$E_\phi = AB_1(\alpha; x) + BH_1(\alpha; x) \quad (11)$$

where A and B are constants. However, E_ϕ must be bounded at the origin thus $B = 0$. The boundary conditions (7) then gives

$$B_1(\alpha; x_0) = 0 \quad (12)$$

where $x_0 = kb$. The eigenvalues of (12) will be denoted by $p_{1,m}(\alpha)$ where the $p_{1,m}(0)$ correspond to the eigenvalues of $J_1(x) = 0$. Figure 5 shows the functional dependence of the first three eigenvalues $p_{1,1}(\alpha)$, $p_{1,2}(\alpha)$ and $p_{1,3}(\alpha)$ on α .

To calculate the propagation constant at given ω and given ferrite parameters we use relations (4), eliminate β to obtain

$$x_0^2(\alpha) = \frac{\omega^2 \mu_o \epsilon b^2 \Delta^2}{1 + [\alpha(1+x)/x]^2} = \frac{x_0^2(0)}{1 + \alpha^2(1+x)^2/x^2} \quad (13)$$

Superposition of the curves generated by (13) on the family of curves $p_{1,m}(\alpha)$, give, for any one value of m , the two sets of values (α, x) that simultaneously satisfy the required conditions (12) and (13). Then, using (4), we may calculate the propagation constants, i.e.,

$$\beta b = \frac{1+x}{x} \cdot \alpha x, \quad (14)$$

It is clear that the curves generated by (13) are symmetric about $\alpha = 0$ and the curves $p_{1,m}(\alpha)$ are not. Thus the propagation constants β_+ and β_- calculated from their points of intersection differ. We observe

that as ω is decreased the guide is 'cut-off' in one direction before the other and the ordinate of (13) approaches $p_{1,m}(0)$. Also, since the slope of $p_{1,m}(\alpha)$ at $\alpha = 0$ is negative and the slope of (13) is zero at $\alpha = 0$ - we see that just prior to 'cut-off' for both directions of propagation there are two intersections of (13) with $p_{1,m}(\alpha)$ for α positive and therefore two distinct modes for the same direction of propagation become possible. These then coalesce as ω is further reduced and complete cut-off is finally reached. The directions of propagation are not identified as forward and reverse since, for α positive, βb may be positive or negative depending on the sign of $(1 + \chi)/\chi$, i.e.,

$$\omega \gtrless [(\gamma H)^2 + \gamma \mu H]^{1/2} \rightarrow (1 + \chi)/\chi \lessgtr 0. \quad (15)$$

We can now treat the case of a circumferentially magnetized ferrite tube mounted coaxially within a circular cylindrical guide. (We again restrict ourselves to considering the rotationally symmetric TE modes). Let the inner and outer radii of the ferrite tube be a and b , respectively, and let d be the guide radius. A cross-section of the guide will then show three regions, namely, an inner region filled by some isotropic dielectric, the middle region containing the ferrite, and an outer region again containing an isotropic dielectric, these regions and related quantities will be identified using the Roman numerals I, II and III for the inner, middle and outer regions.

We can now write the following expressions for the electric field components

$$\begin{aligned} E_{\phi}^I &= E_I J_1(k_o r) e^{-j\beta_I z} \\ E_{\phi}^{II} &= [B_1(\alpha; kr) + CH_1(\alpha; kr)] e^{-j\beta_{II} z} \\ E_{\phi}^{III} &= E_{III} [J_1(k_o r) + DN_1(k_o r)] e^{-j\beta_{III} z} \end{aligned} \quad (16)$$

where

$$k_0^2 = \omega^2 \mu_0 \epsilon - \beta^2 \quad (17)$$

and where E_I , E_{II} , E_{III} , C and D are constants. The dielectric constant of the regions not containing ferrite was taken to be that of the ferrite. This may, in fact, be desirable in practice besides simplifying the calculations somewhat.

Application of the boundary conditions and eliminating the constants yields the transcendental equation

$$\frac{B_1(a; \tau_1 x)}{H_1(a; \tau_1 x)} \cdot \frac{F_1(a; \tau_1 x) - F_2(a; \tau_2 x)}{F_3(a; \tau_1 x) - F_2(a; \tau_2 x)} = \frac{B_1(a; \tau_2 x)}{H_1(a; \tau_2 x)} \cdot \frac{F_1(a; \tau_2 x) - F_2(a; \tau_2 x)}{F_3(a; \tau_2 x) - F_4(a; \tau_2 x)} \quad (18)$$

where

$$F_1(a; \tau x) = [1 - a \tau x + \tau x B_1'(a; \tau x) / B_1(a; \tau x)] / \Delta'$$

$$F_2(a; \tau x) = \tau y J_0(\tau y) / J_1(\tau y)$$

$$F_3(a; \tau x) = [1 - a \tau x + \tau x H_1'(a; \tau x) / H_1(a; \tau x)] / \Delta'$$

$$F_4(a; \tau x) = \tau y Z_0(\tau y) / Z_1(\tau y)$$

and

$$Z_0(\tau y) = J_0(\tau y) N_1(y) - J_1(y) N_0(\tau y)$$

$$Z_1(\tau y) = J_1(\tau y) N_1(y) - J_1(y) N_1(\tau y)$$

where τ may take on the subscripts 1 and 2, and

$$\tau_1 = a/d, \quad \tau_2 = b/d$$

and

$$x = kd, \quad y = k_0 d$$

also

$$E_1(a; y) = \frac{d}{dy} B_1(a; y), \text{ etc.}$$

We have also

$$y^2 = x^2 \{x^2 + [a(1+x)]^2 (1-\Delta')\} / x^2 \Delta' \quad (19)$$

Solutions of the transcendental equation will yield the eigenvalues as a function of a - the intersection of these curves with (19) will then, as before, allow the computation of the propagation constants and the differential phase shift of this structure.

As a sample, and because these results were used in calculations to be presented below, the form that the field components take for the ferrite tube in contact with the guide wall is given.

For $0 \leq r \leq a$ we have

$$\begin{aligned} E_{\phi}^I &= J_1(yr/b) / J_1(\tau y) \\ -j\omega\mu_0 b H_2^I &= y J_0(yr/b) / J_1(\tau y) \\ -j\omega\mu_0 b H_r^J &= jax(1+x) J_1(yr/b) / x J_1(\tau y) \end{aligned} \quad (20)$$

and for $a \leq r \leq b = d$

$$\begin{aligned} E_{\phi}^{II} &= F(a; xr/b) = \frac{B_1(a; xr/b)H_1(a; x) - B_1(a; x)H_1(a; xr/b)}{B_1(a; \tau x)H_1(a; x) - B_1(a; x)H_1(a; \tau x)} \\ -j\omega\mu_0 b H_z^{II} &= \{[b/r - ax] F(a; xr/b) + x F'(a; xr/b)\} / \Delta' \\ -\omega\mu_0 b H_r^{II} &= \{[ax(1+x)/x - xb/(1+x)r] F(a; xr/b) + x F'(a; xr/b)\} / \Delta' \end{aligned} \quad (21)$$

$$F'(a; xr/b) \} / \Delta' ,$$

where the primes indicate differentiation w.r.t. xr/b .

Results and Discussion

As was to be expected for the case of the completely filled guide the curves (Fig. 5) displaying the behavior of the eigenvalues as a function of α are not symmetric about the ordinate since the magnetic intensities in the regions where circular polarization occurs differ, being somewhat stronger nearer the center of the guide. Therefore, even for the completely filled guide a differential phase shift is obtained. This is in contrast to the case of the completely filled rectangular guide.

Figures 6 and 7 show the results of calculations performed on the transcendental equation (18). That is, they show the behavior of the eigenvalues as a function of α for the two limit cases, the ferrite tube collapsed into a central rod and the tube in contact with the guide wall. These calculations were made taking the values $\chi = 0$ and $\chi = .2$, i.e., the magnetizing field H was taken to be zero and $\gamma M/\omega$ was given a representative value of one fifth. The lowest order eigenvalue was calculated for various values of τ where $\tau = a/d$ - thus τ indicates the fraction of the guide cross-section filled with ferrite. In the limit as τ approaches zero or unity these curves approach those for the guide filled completely by an isotropic dielectric or the ferrite. The dielectric constant for both the ferrite and the dielectric regions was taken to be nine.

One would expect that in the partially filled guide the differential phase shift would increase over that of the completely filled guide as, in this case, only one region where circular polarization occurs is contained within the ferrite region. Further, one expects that as τ increases the differentially phase shift increases until τ is such that about half the guide section is filled whereafter it would decrease until it matches the value

for the completely filled guide. Thus, one expects the slope of the eigenvalue curves to be the largest (negatively) when τ is about one half. This is indeed true for α small but as α increases negatively this no longer holds and the curves take a downturn such that in this range the differential phase shift is less than it would be for the completely filled guide. When we have a ferrite tube in contact with the guide wall this effect is even more pronounced (Fig. 7) and we see that for even small α the slopes of the eigenvalue curves are equal to or less than that for the completely filled guide. Of course, for the latter case where the guide contains little ferrite ($\tau \rightarrow 1.$) we expect the eigenvalues curves to become almost symmetric about the ordinate since the differential phase shift will become vanishingly small.

An explanation that would account for the downturn in the eigenvalue curve for α large and negative is that the field must be expelled from the ferrite in this region. To determine if in fact this occurs the components of the electric and magnetic field were computed for this case using (20) and (21) for $\tau = .2$ and $x_0(0) = 6, 20, 30$ and 40 in (13). These values of $x_0(0)$ inserted into (13) assured that the intersection points of (13) with the eigenvalue curve for $\tau = .2$ fell at suitable points, that is, before, on, and after the downturn. The results of these calculations, presented in Figure 8, clearly show that the fields are expelled as α increases negatively - until at $x_0(0)$ equal to about 40 the greater part of the energy is transported for this direction of propagation in the isotropic region. Thus, for this case the magnetic fields are relatively weak throughout the region of circular polarization lying within the ferrite and consequently the anisotropic character of the medium has a smaller effect on the propagation constant for this direction of propagation.

The region of α large and negative holds, in fact, but modest interest since operation in this region would yield decreasing values of differential phase shift. Thus the character of the eigenvalue curves for α above the downtown is of primary interest.

Figure 9 presents a typical curve of the differential phase shift as a function of τ . Again, the explanation of the unexpected result that the maximum differential phase shift occurs for the completely filled guide lies in the fact that the fields show a preference for the isotropic over the anisotropic region. We note that when the guide is about two thirds filled with ferrite ($\tau = .36$) the effect introduced by the region of circular polarization near the guide is exactly counterbalanced by the effect felt due to the ferrite approaching the region of circular polarization near the guide axis.

The final calculations presented here were made to observe the changes in the differential phase shift for a thin tube of ferrite into the guide for various values of the tube mean radius. The computations were made for a ferrite tube of thickness one tenth the guide radius, the parameters X and x again being 0 and .2, respectively, while the remaining guide parameters were selected such that $x_0(0) = 6$. The calculations of the differential phase shift variation with mean tube radius are shown in Figure 10. This graph clearly demonstrates that the differential phase shift increases until the ferrite tube contains a region of circular polarization then decreases, passes through zero, and decreases to a negative maximum when the tube encloses the region circularly polarized in the opposite sense. The fact that the maximum differential phase shift is the greater for the region of polarization nearer the guide axis confirms that the magnetic intensity is the greater there.

Even though the results for the thin tube may be arrived at through perturbation theory the exact solution allows the extension of the calculation to thick tubes and to the investigation of the effect of higher order modes which may yield greatly increased differential phase shift.

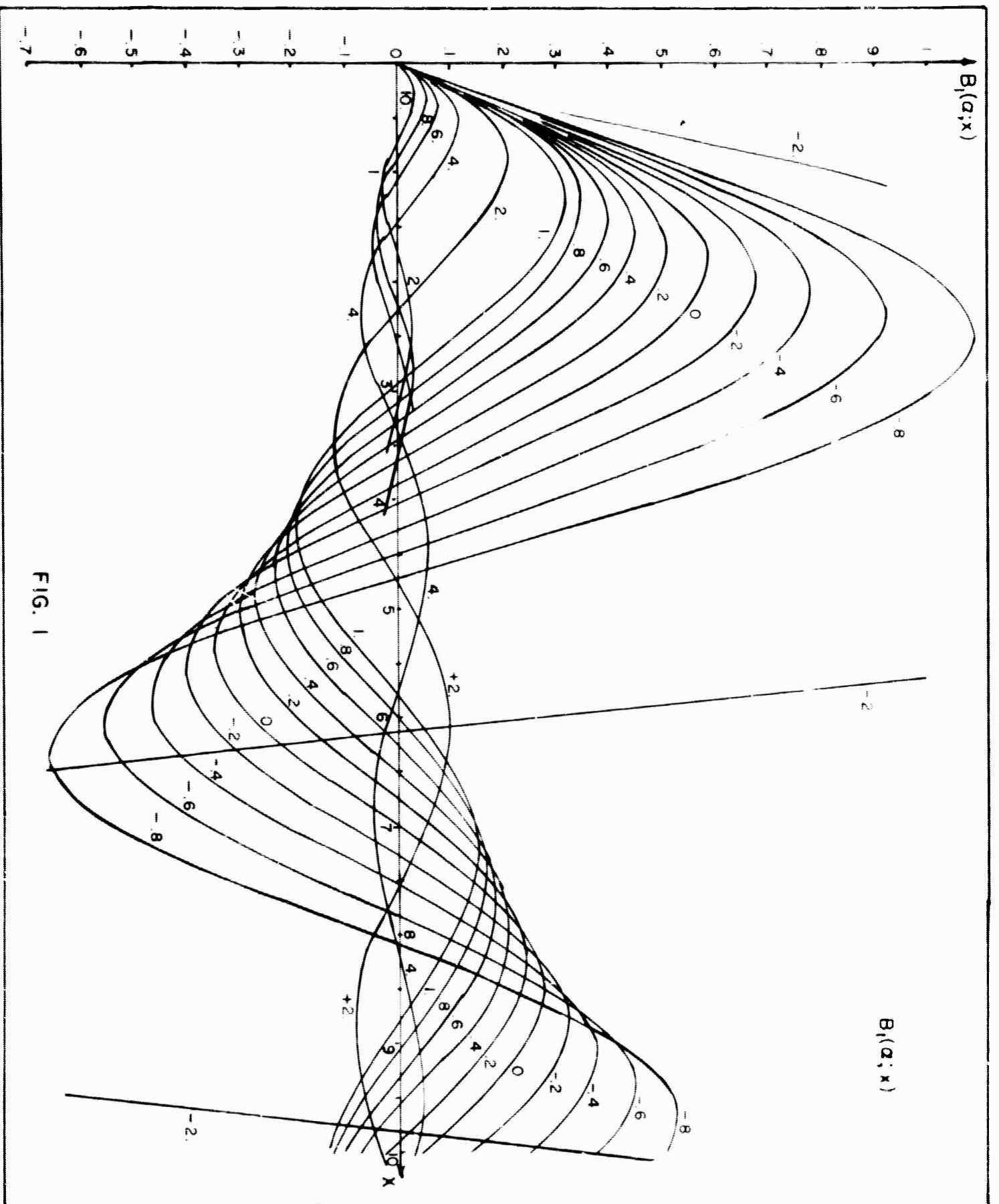


FIG. 1

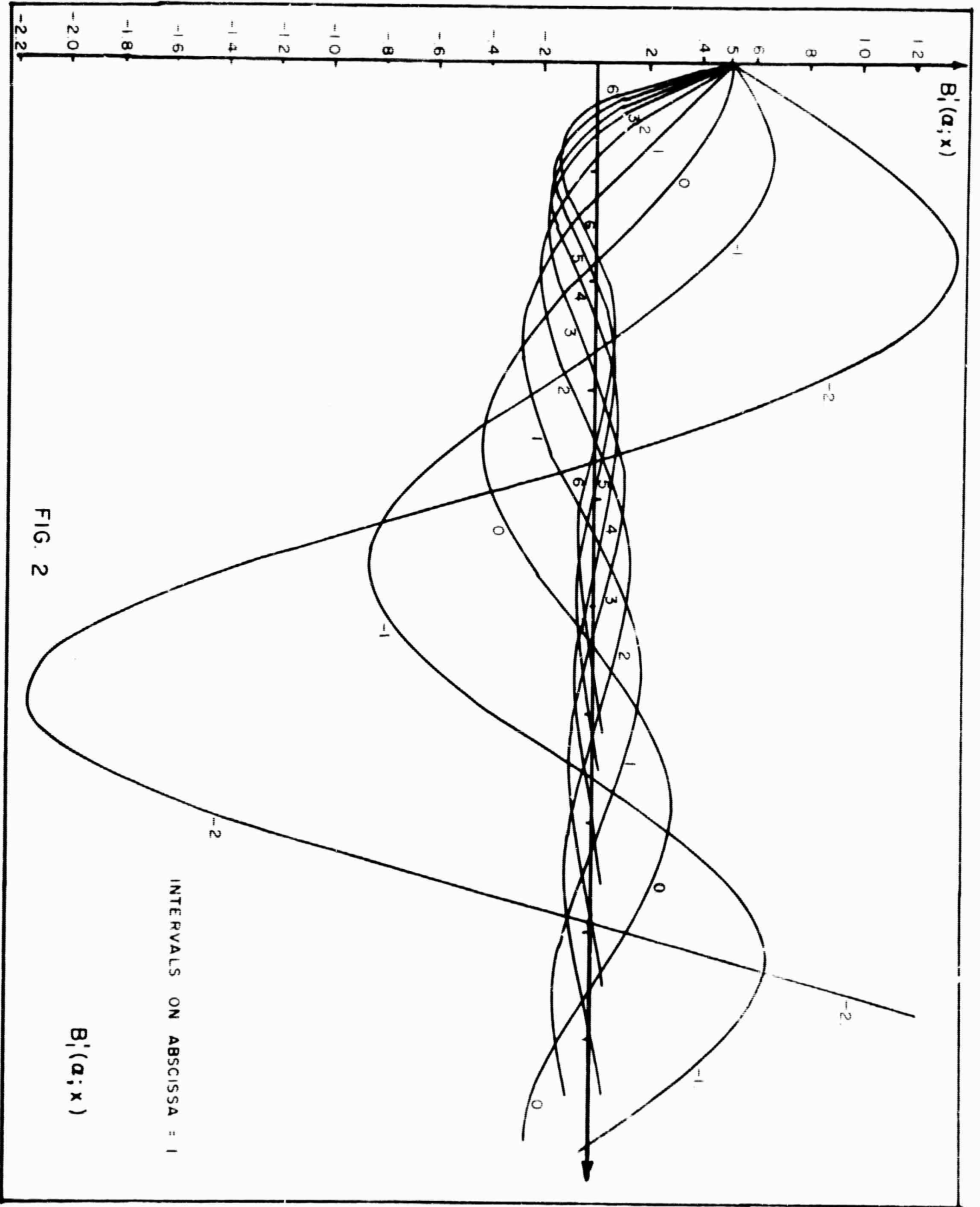


FIG. 2

$B'_i(a; x)$

INTERVALS ON ABSCISSA = 1

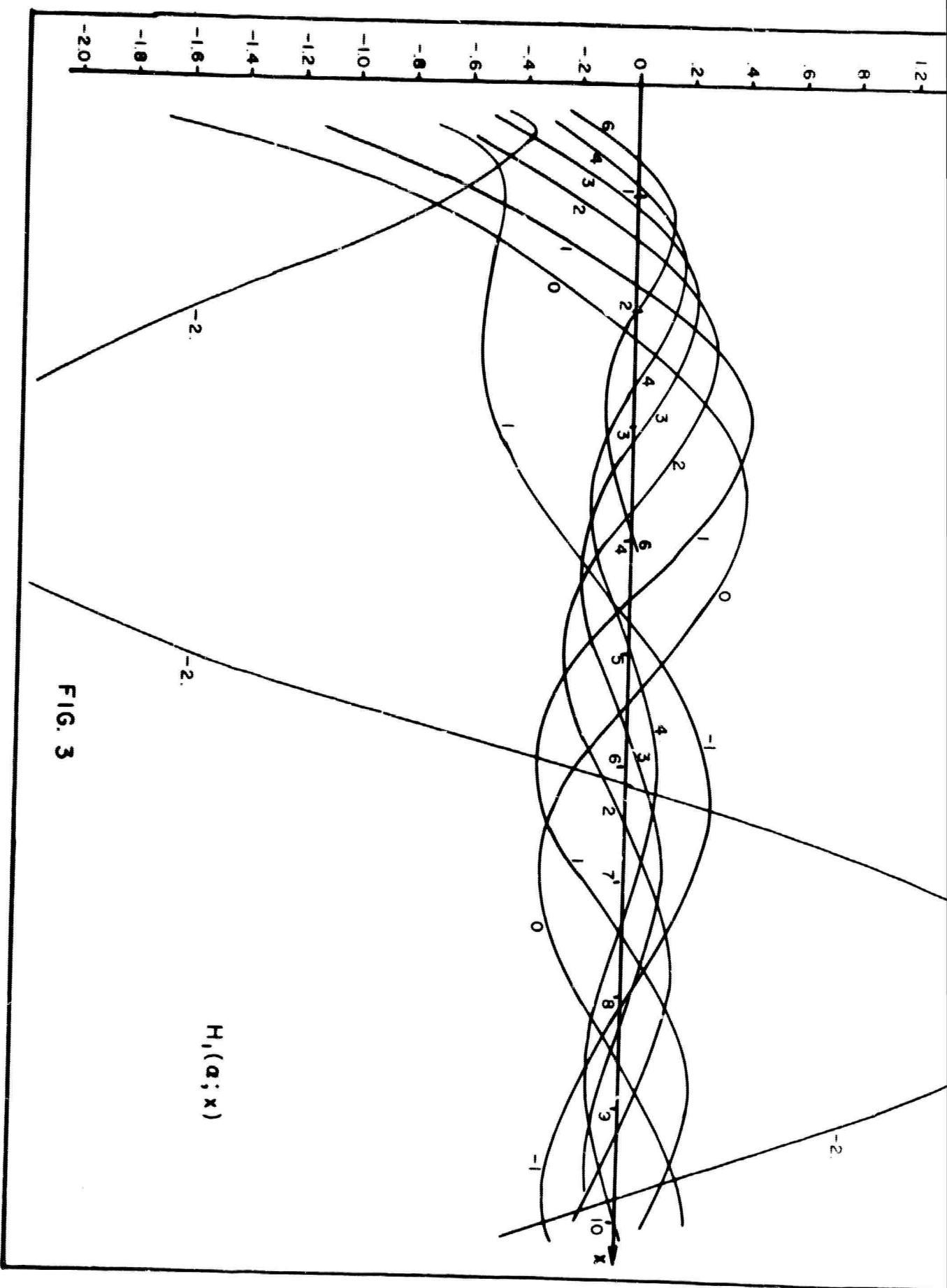


FIG. 3

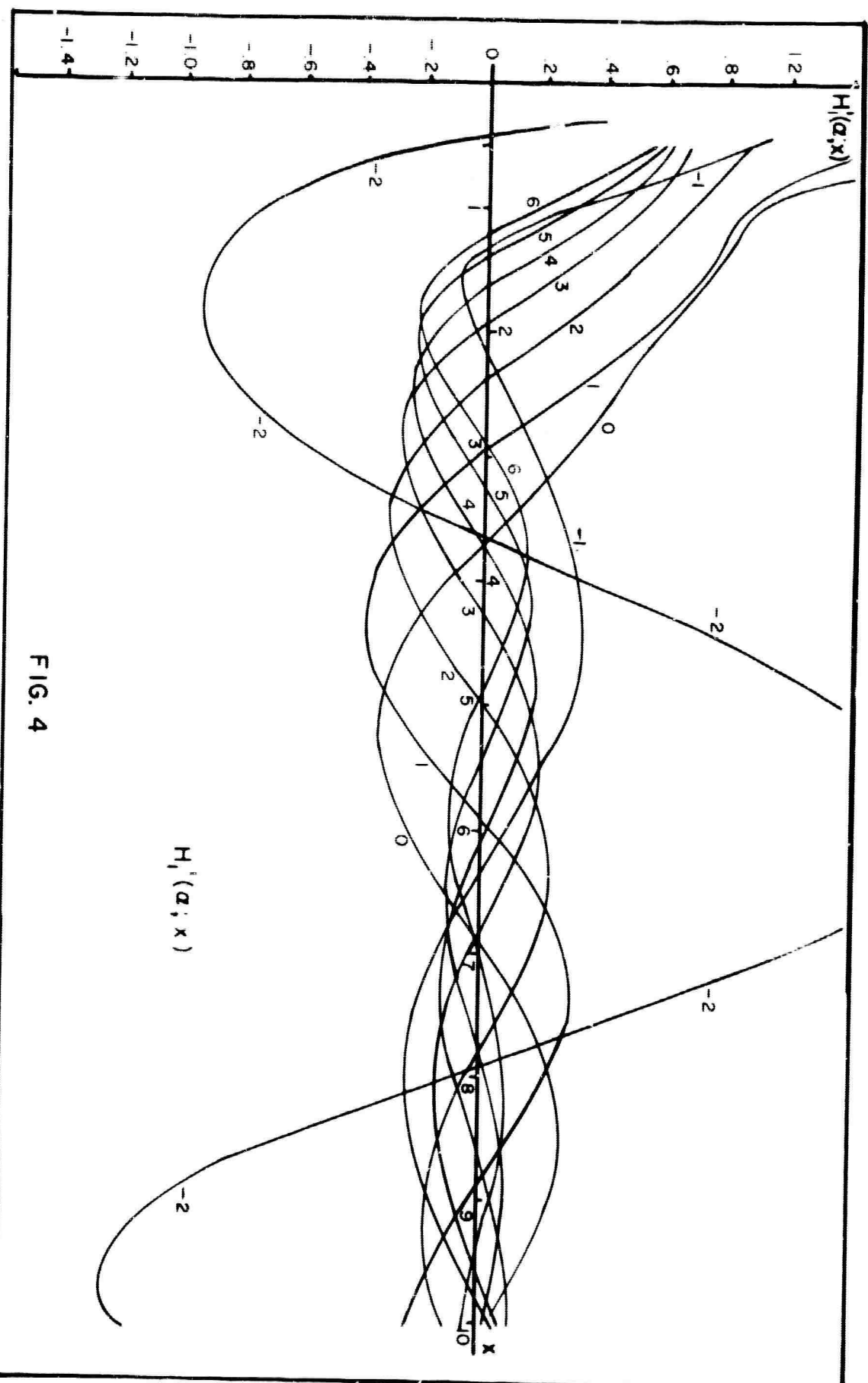


FIG. 4

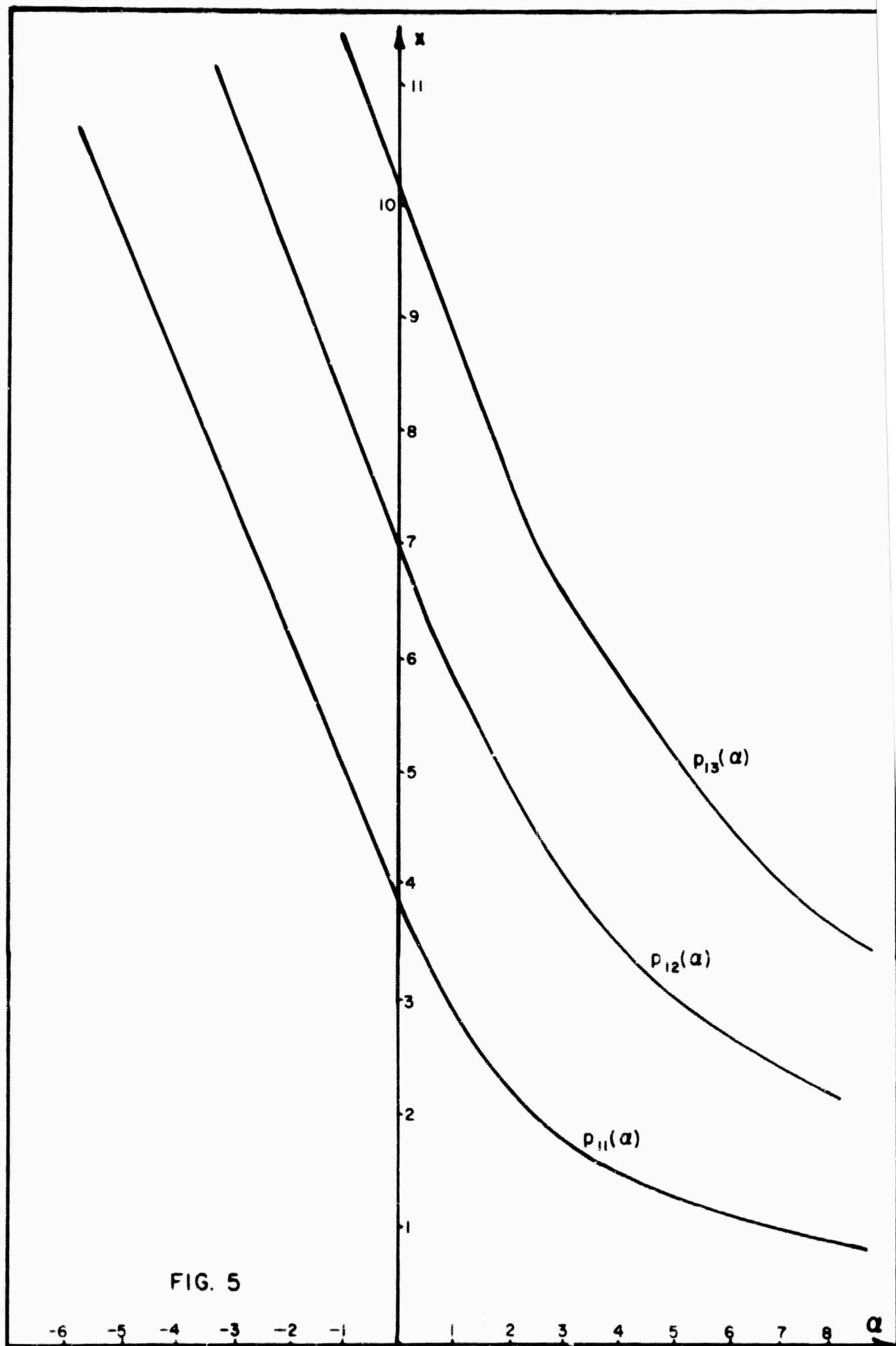
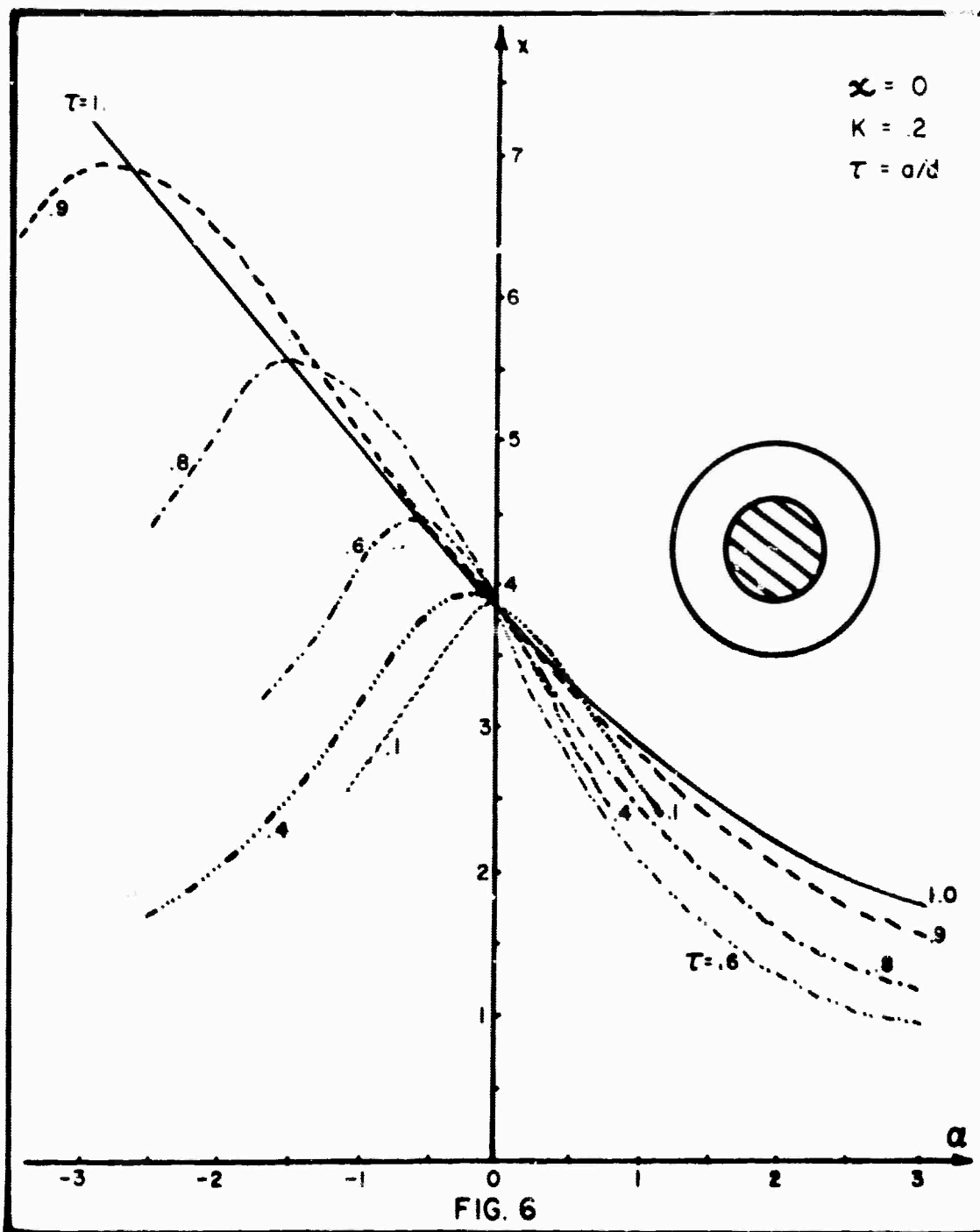
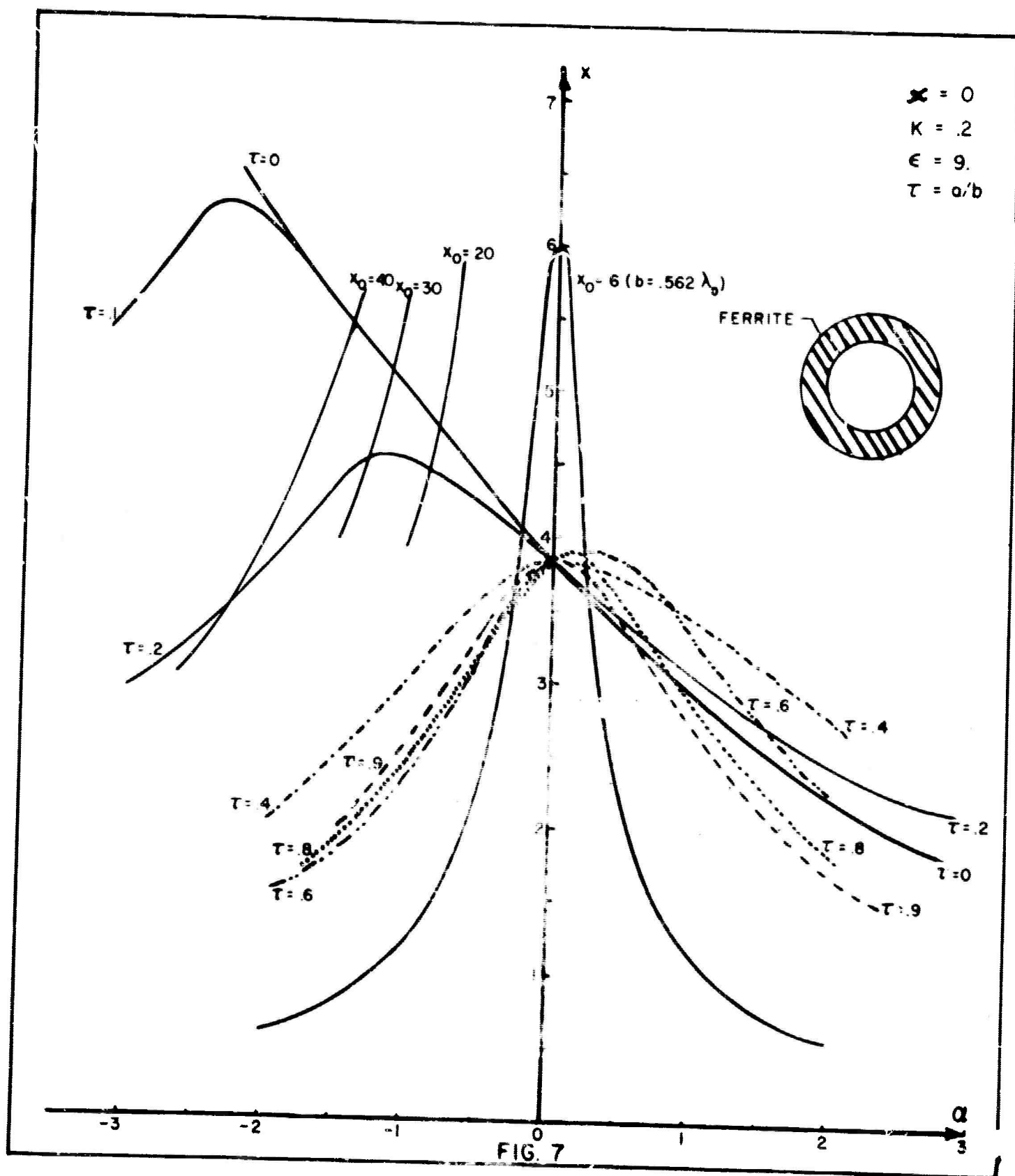


FIG. 5





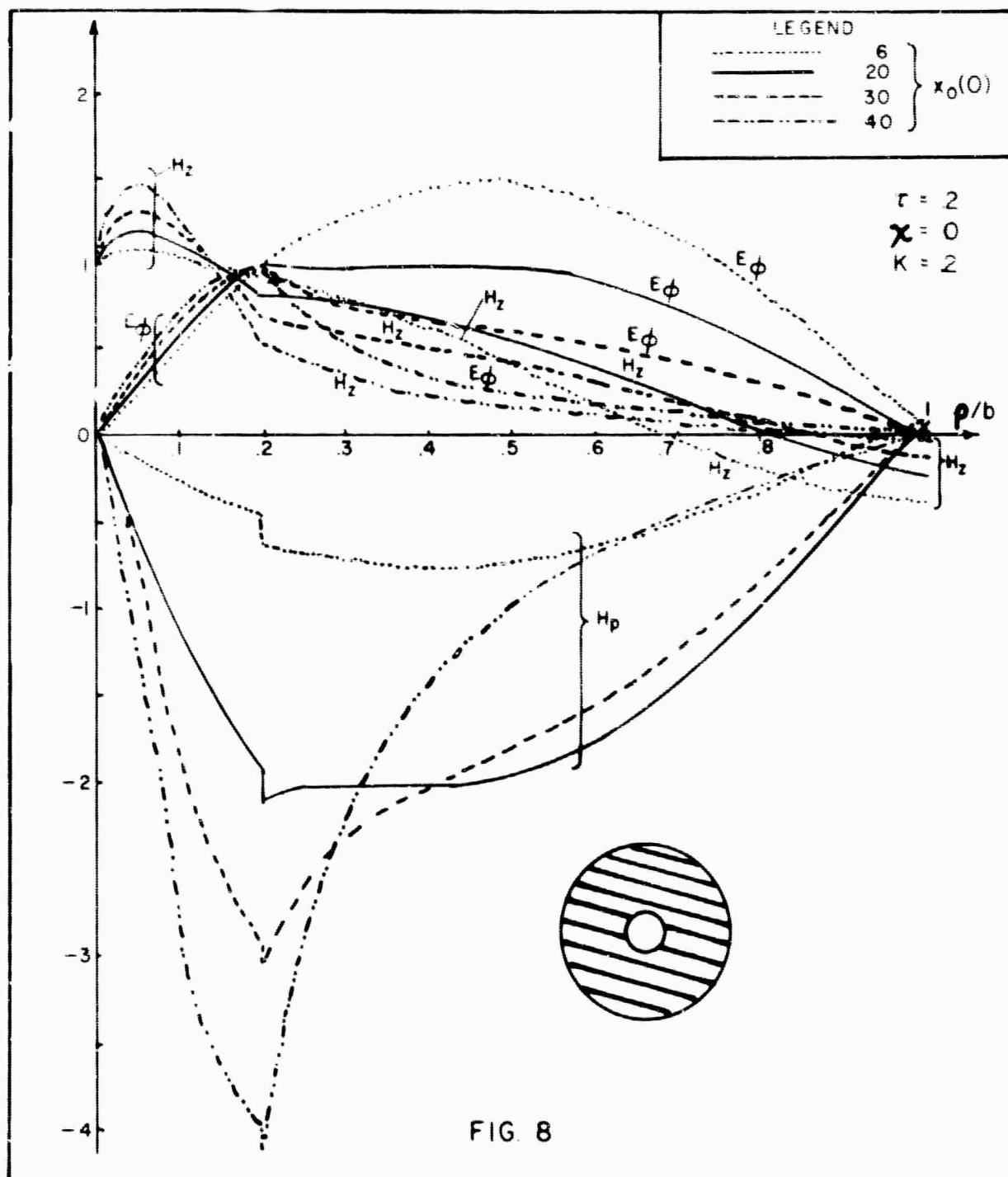
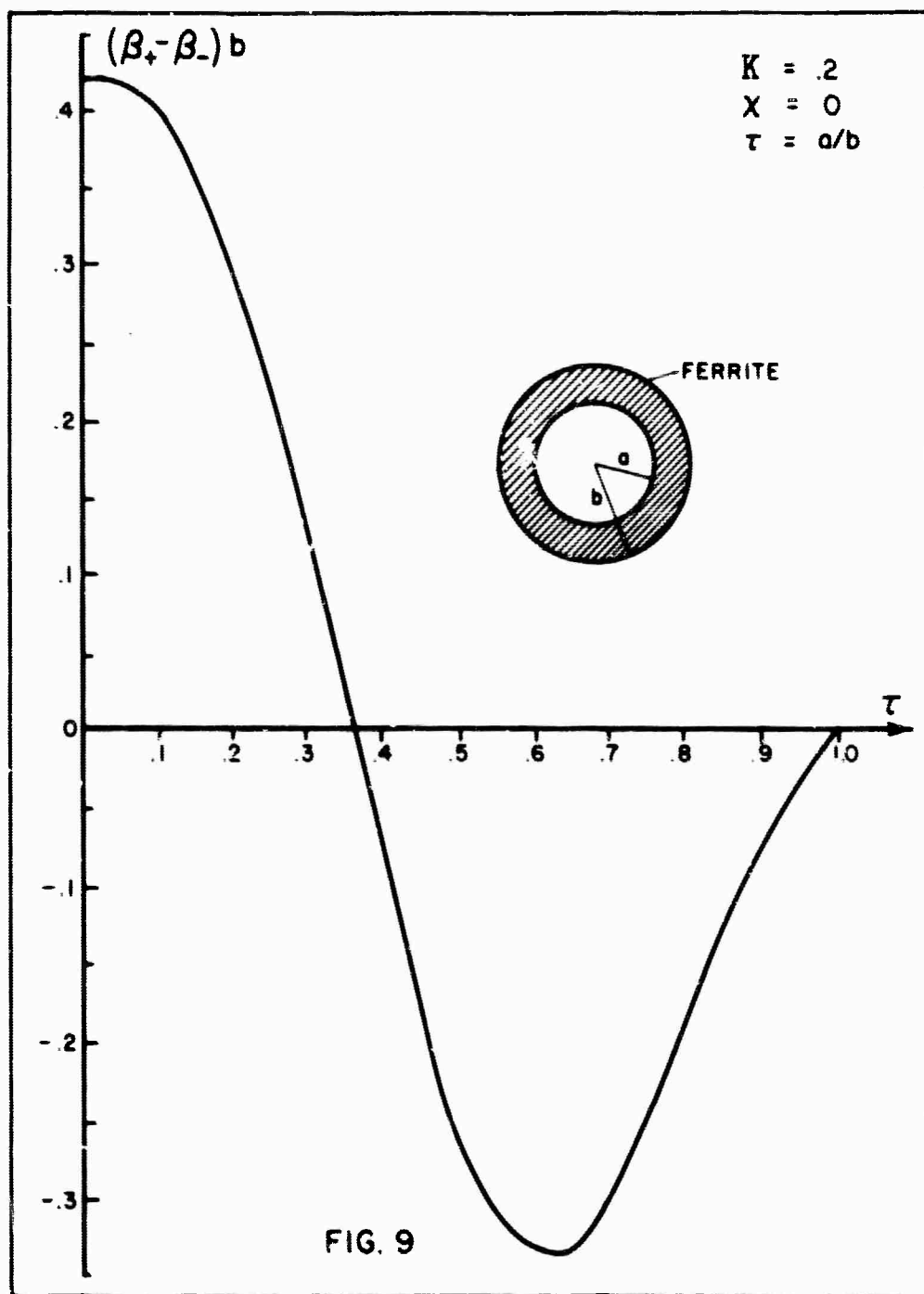


FIG. 8



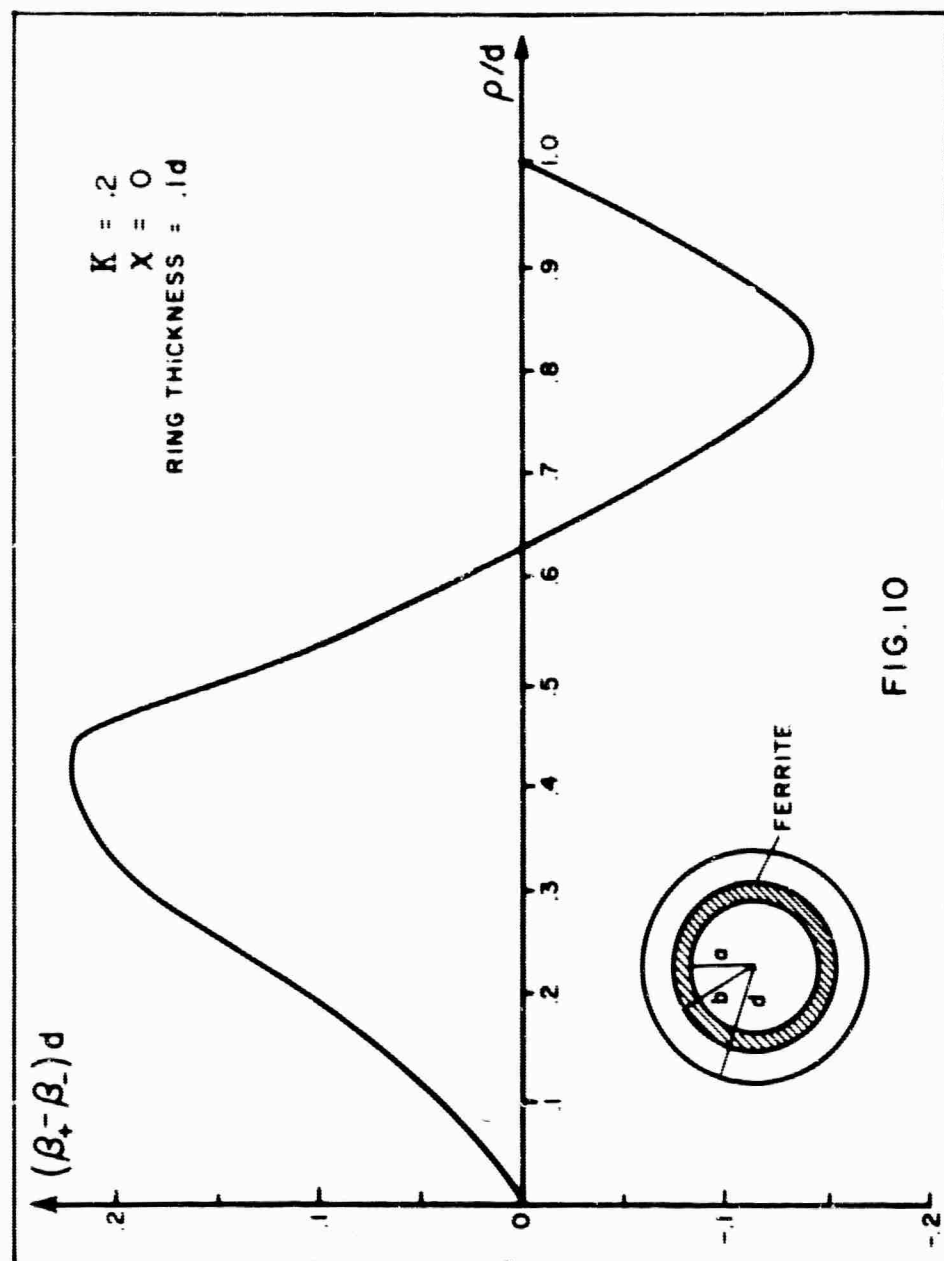


FIG. 10